*Rev. Ivoir. Sci. Technol., 24 (2014) 26 - 44*
*ISSN 1813-3290, http://www.revist.ci*


# INTERFACE CRACK UNDER MIXED MODE I+II LOADING AND INTERNAL SHEAR STRESS DUE TO POISSON EFFECT: THEORY AND CONFRONTATION WITH EXPERIMENTS

**P.N.B. ANONGBA**

*UFR. Sciences des Structures de la Matière et de Technologie, Université FHB. de Cocody, 22 BP 582 Abidjan 22, Côte d'Ivoire*

*Correspondance, e-mail : *anongba@yahoo.fr*

## ABSTRACT

In this study, we analyse an interface crack loaded in mixed mode I + II with an additional internal shear stress that originates from a difference in the magnitudes of the Poisson's contractions present on both sides of the interface. The presence of such an internal shear stress is common in composites under load. The crack is represented by a continuous distribution of two families of edge dislocations with infinitesimal Burgers vectors. The distribution functions of the dislocations at equilibrium satisfy a system of two integral equations with Cauchy-type singular kernels. A solution is given to a class of singular integral equations which, when applied to our modelling, permits to derive closed-form expressions for the dislocation distribution functions and corresponding relative displacements of the faces of the crack, the crack-tip stresses, and the crack extension force. We then proceed to a comparison of theory with experiments with special attention to the work of Liechti and Chai (Journal of Applied Mechanics, 1992) with edge-cracked bi-material epoxy/glass strip specimens in bi-axial loading experiments. Reasonable agreement with experiment is obtained.

**Keywords :** *linear elasticity, poisson effect, dislocations, interface crack, singular integral equations, brittle fracture mechanics.*

**RÉSUMÉ**

**Fissure d'interface sollicitée en mode mixte I+II et en présence d'une contrainte interne de cisaillement promue par l'effet Poisson: analyse théorique et confrontation avec des expériences**

Dans la présente étude, nous analysons une fissure d'interface sollicitée en mode mixte I+II auquel on adjoint une contrainte interne de cisaillement provenant d'une différence dans les valeurs de la contraction de Poisson (perpendiculairement à l'interface) présente de part et d'autre de l'interface. La présence d'une telle contrainte interne est courante dans les matériaux composites en service. La fissure est représentée par une distribution continue de deux familles de dislocations coins de vecteurs de Burgers infinitésimaux. Les fonctions de distribution des dislocations à l'équilibre satisfont un système de deux équations intégrales avec des singularités de type Cauchy. Une solution est proposée pour une certaine classe d'équations intégrales singulières, laquelle appliquée à notre modèle, fournit sous expressions mathématiques fermées, les fonctions de distribution des dislocations de fissure, les déplacements relatifs correspondant des lèvres de la fissure, les contraintes en tête de fissure et la force d'extension de la fissure. Nous procédons ensuite à une confrontation de la théorie avec l'expérience avec une attention particulière aux expériences de Liechti et Chai (Journal of Applied Mechanics, 1992) sur des éprouvettes d'époxy/verre avec encoche sollicitées bi-axialement. Un accord raisonnable avec l'expérience est obtenu.

**Mots-clés :** *élasticité linéaire, effet poisson, dislocations, fissure d'interface, équations intégrales singulières, mécanique de la rupture fragile*.

## I - INTRODUCTION

When two welded dissimilar elastic materials are loaded in tension, perpendicularly to their common interface, an internal shear stress develops. This is the result of a difference in the magnitudes of the Poisson's contractions that are generated in both media. This has been recognized and incorporated recently in the mathematical analysis of the propagation of an interface crack loaded in tension (Anongba [1]); Poisson's effect increases significantly the crack extension force. Consequently, it becomes of interest to discuss Poisson's effect in connection with experiments. A number of experimental studies on the interfacial fracture are available. First, we may mention those using Brazilian disk specimens (Wang and Suo [2], Banks-Sills et al. [3]; Banks-Sills and Ashkenazi [4]; for a review see Banks-Sills [5]).

It is obvious that, for Brazilian disk specimens, when the interface crack is aligned along the applied loading direction (mode I loading), the applied load itself on the specimen disturbs (i.e. inhibits somewhat) the Poisson's contractions about the interface. It thus appears that these tests are not appropriate to evaluate Poisson's effect. Second, we may consider (among others) Liechti and Chai [6,7] which use edge-cracked bi-material (epoxy/glass) strip specimens in biaxial loading experiments; the pair epoxy/glass possesses a large difference in the values of Poisson's contractions on crossing the interface.

An edge-cracked (epoxy/glass) strip specimen under applied tension normal to the interface clearly displays an internal shear stress due to Poisson's effect directed in one direction in the main part of the uncracked region of the specimen ahead of the tip of the starter crack. Hence, applying a shear in the same direction would increase much more the magnitude of the crack extension force whereas in the opposite direction, this would decrease. In the present study, we shall extend our interface crack analysis to bi-axial applied loading (mixed mode I+II) and confront the theoretical findings to experiments with attention to Liechti and Chai [6,7]. The modelling methodology and associated results are given in Section 2 and 3 respectively. Confrontation of the theory with experiments forms Section 4. A conclusion is given in Section 5.

## II - MODELLING METHODOLOGY

### II-1. Internal shear stress on the interface due to Poisson's contraction

Consider two isotropic elastic media (1) and (2) ***(Figure 1),*** isotropic and elastic, with notation $\nu_i$, $\mu_i$, $E_i$ ($i = 1$ and 2) to designate Poisson's ratio, shear modulus and Young's modulus, respectively. We assume that the two solids are firmly linked along a planar interface, such that : mediums 1 and 2 occupy the regions $x_2 > 0$ and $x_2 < 0$ respectively; $Ox_1x_3$ represents the interface with origin *O* at the centre. An interface crack of finite length 2a is present at the origin, extending from $x_1 = -a$ to *a* with a straight front running indefinitely in the $x_3-$direction. ***Figure 1*** has been commented in some details elsewhere [1].

Under the action of a uniform tension $\sigma_{22}^a$, applied at infinity, the solids (1) and (2) suffer a Poisson's contraction of different magnitude; this induces an internal shear stress in the surrounding media about the interface.

For illustration purpose only of the displacement, we construct on the continuum on both sides of the interface an identical cubic lattice. This is not a lattice in the sense of crystallography (i.e. this is not associated with atomic arrangement). We assume that Hooke's law is valid throughout. These lattices are illustrated in dashed lines under the assumption $\nu_2\sigma_{22}^a / E_2 > \nu_1\sigma_{22}^a / E_1$ before the welding of the solids.

Consider two nodes *A* (medium 1) and *B* (medium 2) on either side of the interface which have the equal coordinate $x_1$ (before loading) and a separation distance *d* (along $x_1$) under load when the two materials are not welded. In the welded state, *A* is moved horizontally by a distance of $u_1 < 0$ and *B* by $u_2 > 0$. We ignore vertical displacement along $x_2$. In ***Figure 1***, the displacements $u_1$ and $u_2$ at different places are represented by short horizontal arrows and the resultant welded lattices are partially drawn in solid lines. The induced internal shear stress $\tau_{12}^a$ is represented about the node *A* and is given, at an arbitrary point $P(x_1,0,x_3)$ on the interface, the following expression [1]:

$$\tau_{12}^a(P) = -\frac{\nu_s\mu_s}{a_s}\left(\frac{\nu_1}{E_1} - \frac{\nu_2}{E_2}\right)\sigma_{22}^a x_1 \equiv -\overline{\alpha}x_1 \qquad (1)$$

where $\mu_s$ corresponds to the shear modulus about the interface and $a_s$ is the distance between *A* and *B* along $x_2$ ***(Figure 1)***; $\nu_s = \phi / d$ is the ratio of $\phi$ (distance along $x_1$ between *A* and *B* in the welded state under load) by $d$ (the corresponding distance in the non welded state). $\tau_{12}^a$ is odd function of $x_1$ changing sign in the region $x_1 < 0$ ***(Figure 1).*** When an additional uniform shear stress $\sigma_{12}^a$ is applied externally, the associated displacements in the media amplify or reduce those due to $\tau_{12}^a$ depending on the sign of $\sigma_{12}^a$. In the situation of ***Figure 1*** where $\overline{\alpha} < 0$, positive $\sigma_{12}^a$ amplifies and reduces $\tau_{12}^a$ in $x_1 > 0$ and $x_1 < 0$, respectively.

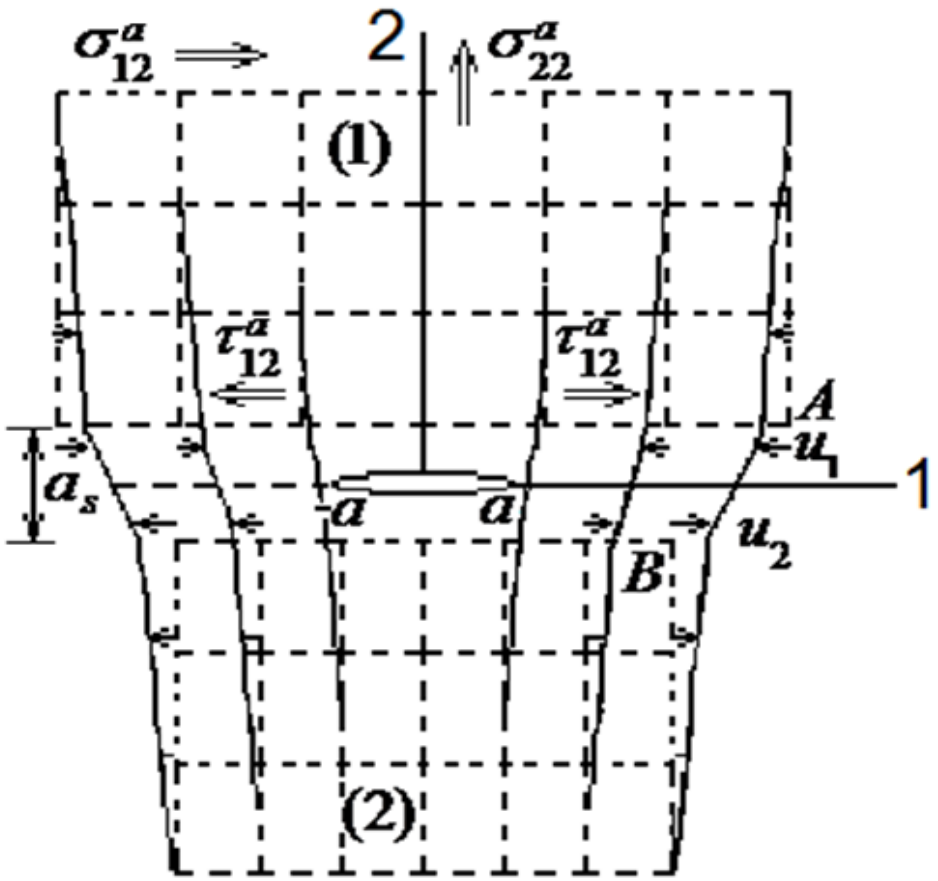


**Figure 1 :** *Two elastic mediums (1) and (2) subjected to a uniform tension* $\sigma_{22}^a$ *at infinity. Far from the interface* $(Ox_1x_3)$*, the mediums suffer uniform Poisson's contractions* $(-\nu_i\sigma_{22}^a / E_i)$ $(i=1$ *and 2) in the* $x_1$ *– direction. The induced shear stress* $\tau_{12}^a$ *is indicated about the interface. A crack of finite length 2a located at the origin is present. This sketch corresponds to* $(\nu_2\sigma_{22}^a / E_2) > (\nu_1\sigma_{22}^a / E_1)$*. For mixed mode I+II loading, an additional applied shear stress* $\sigma_{12}^a$ *is present. In the regions* $x_1 > 0$ *and* $x_1 < 0$*, positive* $\sigma_{12}^a$ *works with and against* $\tau_{12}^a$ *respectively.*

## II-2. Interface crack model and singular integral equations

Our method of analysis consists in representing the crack by a continuous distribution of dislocation families with infinitesimal Burgers vectors (see [1] and additional references therein).

The first step is to determine the distribution functions of the crack dislocation families at equilibrium under load. We generally arrive at a system of singular integral equations involving these functions. When the distribution functions of the dislocations have been found, we can obtain by integration the relative displacements of the faces of the crack, the crack-tip stresses and the crack extension force. The crack in ***Figure 1*** is assumed to be filled with two families (1 and 2) of straight edge dislocations parallel to $x_3$ with Burgers vectors $\vec{b}_1 = (b,0,0)$ and $\vec{b}_2 = (0,b,0)$ in the $x_1$ and $x_2$ directions, respectively. The system is subjected to uniform applied shear $\sigma_{12}^a$ and tension $\sigma_{22}^a$ at infinity; in addition we consider internal shear stresses transmitted by the interface as the result of the existence of internal uniform Poisson stresses $(-\nu_1\sigma_{22}^a)$ and $(-\nu_2\sigma_{22}^a)$ in the $x_1$ – direction in materials 1 and 2, respectively. The dislocation distribution function $D_i(x_1)$ ($i = 1$ and 2) gives the number of dislocations of family *i* in a small interval $dx_1$ about $x_1$ as $D_i(x_1)dx_1$. To find the equilibrium dislocation distributions, we may ask for zero total force on the crack faces; on our modelling, this gives

$$\begin{cases} \bar{\sigma}_{12} = 0 \\ \bar{\sigma}_{22} = 0 \end{cases}; \qquad (2)$$

$\bar{\sigma}_{ij}$ stands for the total stress at any point $P(x_1, x_2, x_3)$ in the surrounding medium and is linked to $D_i$; in (2), we are only concerned with the points of the crack faces. $\bar{\sigma}_{ij}(P)$ is written as

$$\bar{\sigma}_{ij} = \sigma_{ij}^a + \sigma_{ij}^{(s)} + \bar{\sigma}_{ij}^{(1)} + \bar{\sigma}_{ij}^{(2)} \qquad (3)$$

where $\sigma_{ij}^a$ corresponds to both the applied stresses and the assumed uniform internal Poisson stress, $\sigma_{ij}^{(s)}$ to the stress induced by the interface under load in absence of the crack and

$$\bar{\sigma}_{ij}^{(n)} = \int_{-a}^{a} \sigma_{ij}^{(n)}(x_1 - x_1', x_2, x_3) D_n(x_1') dx_1' \quad (n = 1 \text{ and } 2); \qquad (4)$$

here $\sigma_{ij}^{(n)}$ is the stress field produced by a dislocation of family *n* at the origin.

In order to write explicitly (2), we display the following results on the interface (points $P(x_1, x_2 = 0, x_3)$):

- $\sigma_{12}^{(s)}$ is given by $\tau_{12}^{a}$ (1) and $\sigma_{22}^{(s)} \equiv 0$;
- Edges with $\vec{b}_1 = (b,0,0)$ (Family 1)

$$\sigma_{12}^{(1)}(x_1 - x_1^{'}, x_2 = 0, x_3) = \frac{bC}{\pi}\frac{1}{x_1 - x_1^{'}},$$
$$\sigma_{22}^{(1)}(x_1 - x_1^{'}, x_2 = 0, x_3) = -b\beta C\delta(x_1 - x_1^{'}); \qquad (5)$$

- Edges with $\vec{b}_2 = (0,b,0)$ (Family 2)

$$\sigma_{12}^{(2)}(x_1 - x_1^{'}, x_2 = 0, x_3) = b\beta C\delta(x_1 - x_1^{'}),$$
$$\sigma_{22}^{(2)}(x_1 - x_1^{'}, x_2 = 0, x_3) = \frac{bC}{\pi}\frac{1}{x_1 - x_1^{'}}. \qquad (6)$$

In (5) and (6), taken from Comninou and Dundurs [8], $\delta$ is the Dirac delta function. Moreover,

$$C = \frac{2\mu_1(1-\alpha)}{(\kappa_1+1)(1-\beta^2)} = \frac{2\mu_2(1+\alpha)}{(\kappa_2+1)(1-\beta^2)} \qquad (7)$$

with

$$\alpha = \frac{\mu_1(\kappa_2+1) - \mu_2(\kappa_1+1)}{\mu_1(\kappa_2+1) + \mu_2(\kappa_1+1)}; \quad -1 \le \alpha \le 1 \qquad (8)$$

$$\beta = \frac{\mu_1(\kappa_2-1) - \mu_2(\kappa_1-1)}{\mu_1(\kappa_2+1) + \mu_2(\kappa_1+1)}; \quad -\frac{1}{2} \le \beta \le \frac{1}{2} \qquad (9)$$

where $\kappa_i = 3 - 4\nu_i$. The traction free boundary condition (2) yields

$$(\sigma_{12}^{a} - \bar{\alpha}x_1)\delta_{i1} + \sigma_{22}^{a}\delta_{i2} + b\beta C\left(D_2(x_1)\delta_{i1} - D_1(x_1)\delta_{i2}\right) + \frac{bC}{\pi}\int_{-a}^{a}\frac{D_i(x_1^{'})}{x_1 - x_1^{'}}dx_1^{'} = 0, \qquad (10)$$

$i = 1$ and 2, $|x_1| < a$, and $\delta_{ij}$ is the Kronecker delta. We arrive at a system of two integral equations with Cauchy-type singular kernels with unknown functions $D_1$ and $D_2$. The Cauchy principal values of the integrals have to be taken. Next, an analytical solution is given to the governing equations (10).

## III - CALCULATION RESULTS

### III-1. Analytical solution to singular integral equations

From the second of (10) and using the book by Muskhelishvili [9] (see chapter 11 "Inversion formulae for arcs"), we write

$$D_2(x_1) = \frac{1}{\pi bC}\int_{-a}^{a}\sqrt{\frac{a^2 - x_1'^2}{a^2 - x_1^2}}\,\frac{\left(\sigma_{22}^a - b\beta C D_1(x_1')\right)}{x_1 - x_1'}\,dx_1' \qquad (11)$$

Introducing (11) in the first equation of (10), we obtain

$$\int_{-a}^{a}\left(\sqrt{a^2 - x_1^2} - \beta^2\sqrt{a^2 - x_1'^2}\right)\frac{D_1(x_1')}{x_1' - x_1}\,dx_1' = \frac{\pi}{bC}\,f(x_1) \qquad (12)$$

Where

$$f(x_1) = (\sigma_{12}^a - \bar{\alpha}x_1)\sqrt{a^2 - x_1^2} + \beta\sigma_{22}^a x_1\,. \qquad (13)$$

We temporary modify our notation and write (12) as

$$\frac{\sqrt{1-s^2}}{\pi}\int_{-1}^{1}\frac{g(t)}{t-s}\,dt + \frac{\lambda^2}{\pi}\int_{-1}^{1}\frac{\sqrt{1-t^2}\,g(t)}{t-s}\,dt = \frac{1}{abC}\,\bar{f}(s) \qquad (14)$$

Where

$$\begin{aligned} g(t) &= D_1(at) \\ \bar{f}(s) &= f(as) \\ \lambda &= i\beta \end{aligned} \qquad (15)$$

(i. e. $\lambda^2 = -\beta^2$). Equation (14) takes the form of "Example 43" (page 58) in the book by Estrada and Kanwal [10]; by a convincing operational approach , it is shown there that the solution of (14) can be written as

$$g(s) = \frac{\bar{\psi}_1(s) - \bar{\psi}_2(s)}{2\lambda\sqrt{1-s^2}} \qquad (16)$$

where $\bar{\psi}_1$ and $\bar{\psi}_2$ are solutions of the pair of Cauchy type integral equations

$$\overline{\psi}_n(s)+(\delta_{n1}-\delta_{n2})\frac{\lambda}{\pi}\int_{-1}^{1}\frac{\overline{\psi}_n(t)}{t-s}dt=\frac{\bar{f}(s)}{abC}+A\delta_{n1}+B\delta_{n2};\ n=1 \text{ and } 2 \qquad (17)$$

that satisfy the additional requirement

$$\frac{1}{\pi}\int_{-1}^{1}g(t)\ln\left(\frac{1+t}{1-t}\right)dt=\int_{-1}^{1}\frac{\bar{f}(t)}{abC\sqrt{1-t^2}}dt; \qquad (18)$$

$A$ and $B$ are arbitrary constants. The solutions of (17) ($\overline{\psi}_1$ and $\overline{\psi}_2$) can be worked out by using the treatment of Muskhelishvili [9] (see chapter 14 "The case of continuous coefficients"); we have

$$\overline{\psi}_n(s)=\frac{1}{1-\beta^2}\left(\frac{\bar{f}(s)}{abC}+A\delta_{n1}+B\delta_{n2}\right)+(\delta_{n1}-\delta_{n2})\frac{1}{\pi i}\left(\frac{\beta}{1-\beta^2}\right)\left(\frac{1-s}{1+s}\right)^{i\delta(-\delta_{n1}+\delta_{n2})}$$
$$\times\left(const_1\delta_{n1}+const_2\delta_{n2}+\int_{-1}^{1}\frac{\left(\bar{f}(t)/abC+A\delta_{n1}+B\delta_{n2}\right)dt}{(1-t/1+t)^{i\delta(-\delta_{n1}+\delta_{n2})}(t-s)}\right) \qquad (19)$$

where

$$\delta=\frac{1}{2\pi}\ln\left(\frac{1+\beta}{1-\beta}\right); \qquad (20)$$

$n=1$ and 2; $const_1$ and $const_2$ are arbitrary constants. Using (18) and some considerations on the nature (odd and even) of $\bar{f}$ and $g$, we find that (*i*) $const_1=const_2$, $A=-B$ or (*ii*) $const_1=-const_2$, $A=B$. Then, a simple form for $g$ follows from which is deduced the following expression for $D_1$ the distribution function of the edge dislocation family 1:

$$D_1(x_1)=\frac{1}{\pi\sqrt{a^2-x_1^2}}\left(const_1\,\mathrm{Re}\left[\left(\frac{a-x_1}{a+x_1}\right)^{i\delta}\right]+const_2\,\mathrm{Im}\left[\left(\frac{a-x_1}{a+x_1}\right)^{i\delta}\right]\right)$$
$$-\frac{1}{\pi bC\left(1-\beta^2\right)\sqrt{a^2-x_1^2}}\mathrm{Re}\left[\left(\frac{a-x_1}{a+x_1}\right)^{i\delta}\int_{-a}^{a}\left(\frac{a+t}{a-t}\right)^{i\delta}\frac{f(t)}{t-x_1}dt\right], \qquad (21)$$

$-a < x_1, t < a$, Re[...] and Im[...] denote the real and imaginary parts of the complex quantity inside the brackets[ ], and here also, $const_1$ and $const_2$ are arbitrary constants. From $D_1$ (21), we can reach $D_2$ using (11). Closed form solutions are obtained after performing the various integrations in (21) using (13) for *f*. These are given below in the next section assuming zero dislocation content after unloading.

## III-2. Physical quantities associated with the interfacial crack

### *III-2-1. Dislocation distributions; Relative displacements of the faces of the crack*

Closed-form expressions have been obtained for the distribution functions $D_1$ and $D_2$ of the edge crack dislocations. These are

$$D_n(x_1) = \frac{ch(\pi\delta)}{2bC\sqrt{a^2 - x_1^2}} \mathrm{Re}\left[ (i\delta_{n1} + \delta_{n2}) \left\{ 2(\sigma_{22}^a - i\sigma_{12}^a)(x_1 + 2ia\delta) \right.\right.$$
$$\left.\left. - \left(ia^2(1 + 4\delta^2) + 4a\delta x_1 - 2ix_1^2\right)\overline{\alpha} \right\} \left( \frac{a - x_1}{a + x_1} \right)^{i\delta} \right] \qquad (22)$$

$n = 1$ and 2. $D_1$ and $D_2$ only differ by a factor $i$ in front of the curly brackets $\{\ \}$. *ch* is the hyperbolic cosine function. The relative displacement $\phi_n$ ($n = 1$ and 2) of the faces of the crack in the $x_n$ – direction is

$$\phi_n(x_1) = \int_{x_1}^{a} bD_n(x_1')dx_1' \ , \ |x_1| \le a \ , \qquad (23)$$

and after integration

$$\phi_n = \frac{ch(\pi\delta)}{C} \mathrm{Re}\left[ (i\delta_{n1} + \delta_{n2}) \frac{(a - x_1)^{i\delta + 1/2}}{(2a)^{i\delta - 1/2}} \left\{ (\sigma_{22}^a - i\sigma_{12}^a) \left( F(X) - \frac{(a - x_1)F(Y)}{2a(i\delta + 3/2)} \right) \right.\right.$$
$$\left.\left. + 2ia\overline{\alpha} \left( \frac{1 + 2i\delta}{4} F(X) - \frac{a - x_1}{2a(i\delta + 3/2)} \left( i\delta F(Y) + F(Z) \right) \right) \right\} \right], \qquad (24)$$

$n=1$ and 2; $F$ is Gauss's hypergeometric function and $X$, $Y$ and $Z$ are arguments for $F$ with values

$$X=(i\delta+1/2, i\delta+1/2; i\delta+3/2; (a-x_1)/2a)$$
$$Y=(i\delta+1/2, i\delta+3/2; i\delta+5/2; (a-x_1)/2a)$$
$$Z=(i\delta-1/2, i\delta+3/2; i\delta+5/2; (a-x_1)/2a)$$

Other relations of interest (in the calculation of the crack extension force below, for instance) are expressions for $\phi_n$, in the vicinity of the crack tip at $x_1=a$. At the distance $s=a-x_1$, $0<s<<a$, we get using (24)

$$\phi_n(s)=\frac{ch(\pi\delta)\sqrt{2as}}{C}\,\mathrm{Re}\left[(i\delta_{n1}+\delta_{n2})\left(\sigma_{22}^a-i\sigma_{12}^a-a\delta\overline{\alpha}+ia\overline{\alpha}/2\right)\left(\frac{s}{2a}\right)^{i\delta}\right], \quad (25)$$

$n=1$ and 2.

### *III-2-2. Stresses at the crack tip and crack extension force*

We would like to express the total stresses $\overline{\sigma}_{12}$ and $\overline{\sigma}_{22}$ in the plane of the crack in the neighbourhood of the crack tip at $x_1=a$. These are given by the dominant terms of $(\overline{\sigma}_{ij}^{(1)}+\overline{\sigma}_{ij}^{(2)})$ in (3) at point $P=(x_1, x_2=0, x_3)$ with $x_1=a+s_1$, $0<s_1<<a$. Using (3 to 6) and (22) we obtain

$$\overline{\sigma}_{n2}(s_1)=\sqrt{\frac{a}{2s_1}}\,\mathrm{Re}\left[(i\delta_{n1}+\delta_{n2})(1+2i\delta)\left(\sigma_{22}^a-i\sigma_{12}^a-a\delta\overline{\alpha}+ia\overline{\alpha}/2\right)\left(\frac{s_1}{2a}\right)^{i\delta}\right], \quad (26)$$

$n=1$ and 2. A procedure to calculate the crack extension force $G$ has been described by Bilby and Eshelby [11]. We have also referred to it in a number of works [12 to 17]. This gives $G$ as

$$G=\lim_{\Delta a\to 0}\frac{1}{\Delta a}\left(\frac{1}{2}\int_a^{a+\Delta a}\overline{\sigma}_{12}(s_1)\phi_1(s_2)dx_1+\frac{1}{2}\int_a^{a+\Delta a}\overline{\sigma}_{22}(s_1)\phi_2(s_2)dx_1\right); \quad (27)$$

for $\overline{\sigma}_{12}$ and $\overline{\sigma}_{22}$, we use (26) with $s_1=x_1-a$, and for $\phi_1$ and $\phi_2$ (25) with $s_2=a+\Delta a-x_1$. We obtain

$$G = \frac{a\pi(1+4\delta^2)}{4C}\left(\left(\sigma_{22}^{a} - a\delta\overline{\alpha}\right)^2 + \left(\frac{a\overline{\alpha}}{2} - \sigma_{12}^{a}\right)^2\right). \qquad (28)$$

When $G$ is defined as

$$G = G_1 + G_2 \qquad (29)$$

With

$$G_n = \lim_{\Delta a \to 0} \frac{1}{\Delta a}\left(\frac{1}{2}\int_{a}^{a+\Delta a} \overline{\sigma}_{n2}(s_1)\phi_n(s_2)dx_1\right),\ n = 1 \text{and } 2, \qquad (30)$$

it follows

$$G_n = \frac{G}{2} + \left(-\delta_{n1} + \delta_{n2}\right)\frac{ach(\pi\delta)}{4C}$$
$$\times \lim_{\Delta a \to 0} \mathrm{Re}\left[(1+2i\delta)\eta^2 B\left(i\delta + 3/2, i\delta + 1/2\right)\left(\frac{\Delta a}{2a}\right)^{2i\delta}\right],\ n = 1 \text{and } 2, \qquad (31)$$

Where

$$\eta = \sigma_{22}^{a} - i\sigma_{12}^{a} - a\delta\overline{\alpha} + ia\overline{\alpha}/2; \qquad (32)$$

$B(x, y)$ is the beta function (Euler's integral of the first kind). It thus appears that $G$ (28) is well defined, but $G_n$, associated with individual loading modes I and II, carries an oscillatory term with $\Delta a$ indefinitely. The crack extension force possesses the following aspects:

- $G$ (28) the total energy release rate is well defined,
- $G_1$ and $G_2$ (30) the individual energy release rates associated with modes II and I carry an oscillatory term with $\Delta a$ indefinitely,
- If the oscillatory term is neglected, then $G_1 = G_2 = G/2$ (31).

These behaviours of the crack extension force have been described earlier by Sun and Jih [18] and Raju et al. [19].

## IV - CONFRONTATION WITH EXPERIMENTS

Experimental works provide the crack extension force (i.e. fracture toughness) as a function of phase angle, also termed mode mix or mixity ([2 to 7], among others). The phase angle $\psi$ at position $P=(x_1, x_2=0, x_3)$, on the interface ahead of the crack front, with $x_1 = a + s_1$, $0 < s_1 << a$, is defined in terms of crack-tip stresses as

$$\psi = \tan^{-1}\left(\bar{\sigma}_{12}(s_1)/\bar{\sigma}_{22}(s_1)\right). \tag{33}$$

Making use of (26), we write

$$\tan\psi = -\frac{x_0 \tan\theta_1 + y_0}{x_0 - y_0 \tan\theta_1} \tag{34}$$

where

$$\begin{aligned} \theta_1 &= \delta \ln(s_1/2a), \\ x_0 &= \sigma_{22}^a\left(1 - 2\delta\kappa_s\tilde{a} + 2\delta M\right), \\ y_0 &= \sigma_{22}^a\left(2\delta + (1-4\delta^2)\kappa_s\tilde{a}/2 - M\right) \end{aligned} \tag{35}$$

with $\kappa_s = \nu_s\mu_s(\nu_1/E_1 - \nu_2/E_2)$, $\tilde{a} = a/a_s$ and $M = \sigma_{12}^a/\sigma_{22}^a$. The crack extension force $G$ (28) can be expressed in terms of the phase angle as

$$G = \left(1-\delta\kappa_s\tilde{a}\right)^2 G\left(M=0;\kappa_s=0\right)\frac{(1+4\delta^2)(1+\tan^2\theta_1)(1+\tan^2\psi)}{\left(1-2\delta\tan\theta_1-(2\delta+\tan\theta_1)\tan\psi\right)^2} \tag{36}$$

Where

$$G\left(M=0;\kappa_s=0\right) = \frac{a\pi(1+4\delta^2)\sigma_{22}^{a\ 2}}{4C}. \tag{37}$$

$G(M=0;\kappa_s=0)$ is the value of the crack extension force when both $M$ (the applied shear by tension ratio) and $\kappa_s$ are zero. From (1), it may be seen that $\kappa_s = 0$ corresponds to $\tau_{12}^a = 0$ (absence of Poisson's effect). Poisson's effect is taken into account only when $\kappa_s \neq 0$. Other relations are of interest. We first mention the relation between $M$ and the phase angle $\psi$; this is derived from (34) as

$$M = \frac{A_1 + B_1 \tan\psi}{1 - 2\delta \tan\theta_1 - (2\delta + \tan\theta_1)\tan\psi} \qquad (38)$$

Where

$$A_1 = 2\delta + (1 - 4\delta^2)\kappa_s \tilde{a}/2 + (1 - 2\delta\kappa_s \tilde{a})\tan\theta_1,$$
$$B_1 = 1 - 2\delta\kappa_s \tilde{a} - (2\delta + (1 - 4\delta^2)\kappa_s \tilde{a}/2)\tan\theta_1.$$

It is also interesting to mention the following result on the value of the phase angle at the minimums of the crack extension force. When $\kappa_s = 0$, $G$ (28) is minimum for $M = 0$ (i.e. $\sigma_{12}^a = 0$ ); this minimum corresponds to $G(M = 0; \kappa_s = 0)$ (37). When $\kappa_s \neq 0$ , $G$ (28) is minimum for $M = \kappa_s \tilde{a}/2 \equiv M_E$ with value

$$G_E = (1 - \delta\kappa_s \tilde{a})^2 G(M = 0; \kappa_s = 0). \qquad (39)$$

It is noted that both minimums of $G$ correspond to the equal phase angle $\psi_E$ (use (34) for instance) given by

$$\tan\psi_E = -\frac{2\delta + \tan\theta_1}{1 - 2\delta\tan\theta_1}. \qquad (40)$$

$\psi_E$ depends on $\theta_1 = \delta \ln(s_1/2a)$ and therefore on the values given to $s_1$ and $a$. For illustration purpose and to confront theory with experiments, we consider the work of Liechti and Chai [7] with the bi-material system (1)/(2) of our modelling corresponding to the pair epoxy/glass. The parameters taken from their work are:

$\delta = -0.0605$; $E_1 = 2.03$ GPa, $\nu_1 = 0.37$; $E_2 = 68.95$ GPa, $\nu_2 = 0.20$.
We also use $E_i = 2\mu_i(1 + \nu_i)$ and take $\mu_s = (\mu_1 + \mu_2)/2$, $\nu_s = 0.5$ (see [1]).

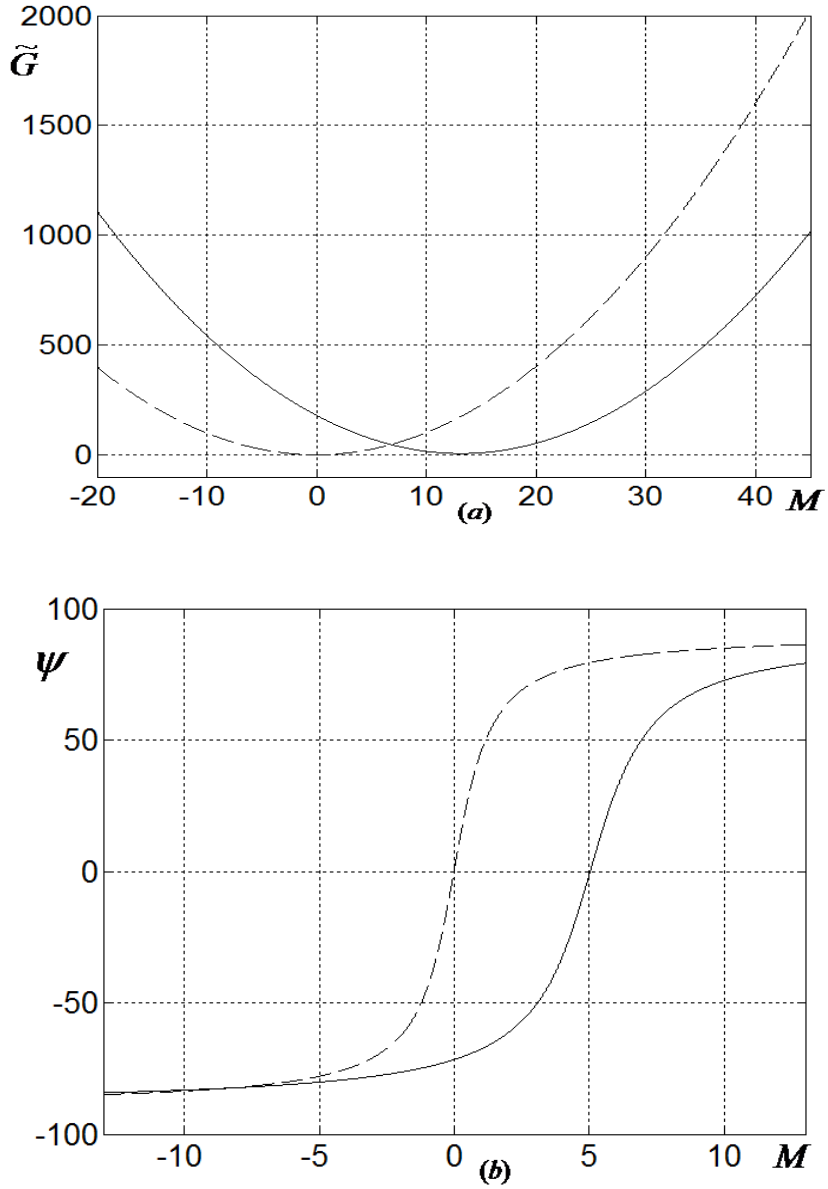


**Figure 2 :** *(a) Reduced crack extension force* $\tilde{G} = G / G(M = 0; \kappa_s = 0)$ *as a function of* $M = \sigma_{12}^a / \sigma_{22}^a$, $\tilde{a} = 20$. *(b) Phase angle* $\psi$ *(degrees) as a function of* $M$. *The identical* $\psi_E (= 0.67°)$ *corresponds to both* $M = 0$ $(\kappa_s = 0)$ *and* $M = M_E = 5.04$ $(\kappa_s \neq 0)$; $2a = 7.65$ cm, $s_1 = 1.27$ cm, $a_s = 0.5$ cm.

In both (a) and (b), dashed and solid curves corresponds to $\kappa_s = 0$ and $\kappa_s \neq 0$ respectively; material parameters for the system (1)/(2) correspond to epoxy/glass (see text).

***Figure 2a*** is a graphical representation of $\tilde{G}$, the crack extension force $G$ (28) reduced by $G(M=0;\kappa_s=0)$ (37), as a function of $M=\sigma_{12}^a/\sigma_{22}^a$. When $\kappa_s=0$, $\tilde{G}$ is minimum for $M=0$; when Poisson's effect is taken into account ($\kappa_s\neq 0$), this minimum is shifted to $M=\kappa_s\tilde{a}/2\equiv M_E$ (see below (35) for $\tilde{a}$). The reduced $\tilde{G}$ increases indefinitely when $M$ moves away from $M_E$ along the opposite directions. If one takes $2a=7.65$ cm (the length of the edge starter crack of the specimens [7]) and $a_s=0.5$ cm ($\tilde{a}=a/a_s=7.65$), this gives $M_E=5.04$.

***Figure 2b*** represents the phase angle $\psi$ as a function of $M$ (using (38)). Here also, dashed and solid curves corresponds to $\kappa_s=0$ and $\kappa_s\neq 0$ respectively. We take values close to those of Liechti and Chai [7]: $2a=7.65$ cm and $s_1=1.27$ cm; this gives $\psi_E=0.67°$, $M_E=5.04$. As mentioned earlier $\psi_E$ corresponds to $M=0$ on the $\kappa_s=0$ curve and $M=M_E$ on the $\kappa_s\neq 0$ curve.

For the system (1)/(2) corresponding to the epoxy/glass, $\tau_{12}^a$ (1) is negative in the $x_1>0$ region of the fracture specimen; this means that positive $M$ reduces the internal strain caused by $\tau_{12}^a$ while negative $M$ amplifies this strain in that region. For $\kappa_s\neq 0$ (solid curve in ***Figure 2b***) and $M=0$, the phase angle is negative with a large magnitude (about -70°); with increasing positive applied $M$, the phase angle $\psi$ increases drastically: $M$ interval of [0, 10] corresponds to $\psi$ interval of [-70°, 70°] approximately. The corresponding decrease of $\psi$ for negative $M$ is much less pronounced: $M$ interval of [-20, 0] for $\psi$ interval of [-85°, -72°] approximately. For the experimentalist, starting from zero applied $M$, this is the manifestation of an apparent asymmetry. Edge-cracked bi-material strip specimens in bi-axial loading experiments would display an asymmetrical behaviour with respect to the direction of the applied shear stress $\sigma_{12}^a$ as may be noted in [7]. We further defined from (36) $\hat{G}(\psi)$ as

$$\hat{G}=\frac{G}{\left(1-\delta\kappa_s\tilde{a}\right)^2 G\left(M=0;\kappa_s=0\right)}=\frac{(1+4\delta^2)(1+\tan^2\theta_1)(1+\tan^2\psi)}{\left(1-2\delta\tan\theta_1-(2\delta+\tan\theta_1)\tan\psi\right)^2}. \quad (41)$$

***Figure 3*** represents $\hat{G}(\psi)$ for $2a=7.65$ cm and $s_1=1.27$ cm. Also reported are experimental values (symbol $*$) of the fracture toughness versus phase angle $\psi$ given by Liechti and Chai [7] (their ***Figure 6***).

What we do first is to identify (by simple inspection) the minimum value: we find it to be located at $\psi_m = 20°$, approximately. We then report the experimental data so that $\psi_m$ be read $\psi_E$ (40); with the values given to *a* and $s_1$ above, $\psi_E = 0.67°$. Hence for each value of the phase angle provided by Liechti and Chai [7], we add the negative value $\psi_E - \psi_m$; then, the experimental fracture toughness is reduced by 3.75 J/m$^2$ (taken as the associated minimum). Comparison between $\hat{G}$ (41) and experimental points (symbol $*$) seems quite satisfactory. We use $\hat{G}$ instead of $\tilde{G} = G/G(M=0;\kappa_s=0)$ because Liechti and Chai [7] didn't take any account of Poisson's effect in their considerations with theory. Taking into account Poisson's effect would require to multiply the fracture toughness values in ***Figure 3*** by the quantity $(1-\delta\kappa_s\tilde{a})^2$ (see (36)); with $a_s = 1/2$ cm

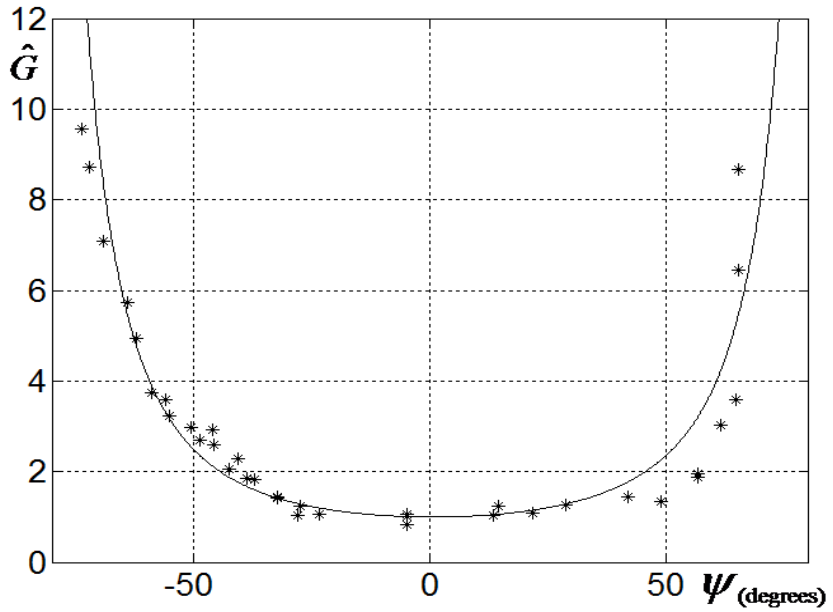


**Figure 3 :** *Reduced crack extension force $\hat{G}$ (41) (solid curve) as a function of phase angle $\psi$ (degrees). Experimental points (symbol $*$) are those of Liechti and Chai (1992) (their Fig. 6); $2a = 7.65$ cm, $s_1 = 1.27$ cm and material parameters correspond to epoxy/glass (system(1)/(2)) (see text).*

And $2a = 7.65$ cm ( $\tilde{a} = 7.65$ ) and epoxy/glass, this gives the value 2.6 approximately. In other words, we would consider $\tilde{G}$ instead of $\hat{G}$.

We also note that our crack model of ***Figure 1*** is different from the edge-cracked bi-material system in [7] (see their ***Figure. 1***); however this difference seems not too serious in the graphical representation of fracture toughness versus phase angle, on view of ***Figure 3***.

## V - CONCLUSION

The mathematical analysis of a bi-material interface crack of finite length 2*a* under applied mixed mode I+II loading, incorporating an internal shear stress that originates from a difference in Poisson's contractions on crossing the interface, has been performed. Various physical quantities, involved in the discussion of the conditions for crack motion, are given in closed-form expressions. These are the relative displacement of the faces of the crack, the crack-tip stress and the crack extension force. This would help to a better interpretation of experimental findings in a number of situations. Confrontation with experiments has been done with attention to the work of Liechti and Chai (1992) with edge-cracked bi-material epoxy/glass strip specimens in bi-axial loading experiments.

## REFERENCES

[1] – P.N.B. ANONGBA, Rev. Ivoir. Sci. Technol., 23 (2014) 54 - 71.

[2] – J.-S. WANG and Z. SUO, Acta Metall. Mater., 38 (1990) 1279 - 1290.

[3] - Int. J. Fract., 99 (1999) 143 - 160.

[4] - L. BANKS-SILLS and D. ASHKENAZI, Int. J. Fract., 103 (2000) 177 -188.

[5] - L. BANKS-SILLS, Strain, 50 (2014) 98 - 110.

[6] - K.M. LIECHTI and Y.-S. CHAI, J. Appl. Mech., 58 (1991) 680 - 687.

[7] - K.M. LIECHTI and Y.-S. CHAI, J. Appl. Mech., 59 (1992) 295 - 304.

[8] - M. COMNINOU and J. DUNDURS, J. Elasticity, 10 (1980) 203 - 212.

[9] - N.I. MUSKHELISHVILI, "Singular integral equations", Dover Publications, New York (1992).

[10] - R. ESTRADA and R.P. KANWAL, "Singular integral equations", Birkhäuser, Boston (2000).

[11] - B.A. BILBY and J.D. ESHELBY, In: "Fracture", Ed. Academic Press (H. Liebowitz), New York, Vol 1 (1968) 99 - 182.

[12] - P.N.B. ANONGBA, Physica Stat. Sol. B, 194 (1996) 443 - 452.

[13] - P.N.B. ANONGBA, Int. J. Fract., 124 (2003) 17 - 31.

[14] - P.N.B. ANONGBA, Rev. Ivoir. Sci. Technol., 14 (2009) 55 - 86.

[15] - P.N.B. ANONGBA, Rev. Ivoir. Sci. Technol., 16 (2010) 11 - 50.

[16] - P.N.B. ANONGBA, J. BONNEVILLE and A. JOULAIN, Rev. Ivoir. Sci. Technol., 17 (2011) 37 - 53.

[17] - P.N.B. ANONGBA and V. VITEK, Int. J. Fract., 124 (2003) 1 - 15.

[18] - C.T. SUN and C.J. JIH, Eng. Fracture Mech., 28 (1987) 13 - 20.

[19] - J.S. RAJU, J.H. CREWS and M.A. AMINPOUR, Eng. Fracture Mech., 30 (1988) 383 - 396.